



Comment on “Theory of phonon-assisted adsorption in graphene: Many-body infrared dynamics”

 Dennis P. Clougherty 

*JILA, National Institute of Standards and Technology, University of Colorado, 440 UCB, Boulder, Colorado 80309, USA
and Department of Physics, University of Vermont, Burlington, Vermont 05405-0125, USA*

 (Received 30 September 2019; accepted 11 May 2020; published 11 June 2020)

Two approximations used by Sengupta [Phys. Rev. B **100**, 075429 (2019)] in numerically computing the adsorption rate of cold hydrogen atoms on suspended graphene are critically examined. The independent boson model approximation (IBMA) was used to compute the atom self-energy, and the single-pole approximation (SPA) was used to obtain the adsorption rate from the self-energy. It is shown explicitly that there are additional contributions to the self-energy appearing at the same order of the atom-phonon coupling as the IBMA terms that alter the value of the real part of the self-energy at low energies by several orders of magnitude in the regime of interest. This shift in the self-energy, consequently, renders the use of SPA invalid.

DOI: [10.1103/PhysRevB.101.247401](https://doi.org/10.1103/PhysRevB.101.247401)

The work of Ref. [1] revisits a physisorption model proposed by Clougherty [2] to describe the effects from the infrared (IR) phonon dynamics on sticking to two-dimensional materials. Ref. [1] relies on the assumption that the self-energy of the slow incident atom can be approximated by the one-loop diagram where the atom propagator is replaced by the propagator of the independent boson model (IBM), an approximation, henceforth, referred to as the independent boson model approximation (IBMA). This approximation was not derived; consequently, the regime of validity for the IBMA was not obtained.

Using the IBMA self-energy, the sticking rate is calculated numerically by evaluating the imaginary part of the IBMA self-energy at the atom energy E_k . This single-pole approximation (SPA) to the real-time atom Green's function rests on a number of assumptions about the behavior of the self-energy [3]. Additionally, Ref. [1] finds the quasiparticle weight as $Z \approx 0.99$ for all atom energies E_k considered.

From numerical results based on these approximations, Ref. [1] concludes that, for suspended micromembranes of graphene at $T = 10$ K, the adsorption rate will be finite, independent of the membrane size, and in agreement with the lowest-order perturbative result obtained by Fermi's golden rule. This conclusion is in disagreement with two previous theoretical studies that concluded at low atom energies the sticking rate is severely suppressed by a phonon orthogonality catastrophe [2,4–6].

In this Comment, the two approximations of Ref. [1] are critically examined. To assess the validity of the IBMA, the exact closed-form expression for the atom self-energy to quadratic order in the atom-phonon coupling [$O(g_{kb}^2)$] is obtained. This order $O(g_{kb}^2)$ self-energy includes many contributions neglected in the IBMA. This result is then compared to the IBMA self-energy for parameter values used in Ref. [1]. Finally, the $O(g_{kb}^2)$ self-energy is used to examine the validity of SPA in approximating the adsorption rate.

Using the model of Eqs. (1)–(3) in Ref. [1], the exact atom self-energy to order $O(g_{kb}^2)$ is

$$\Sigma(t) = -ig_{kb}^2 \sum_{m,n} \langle T[X(t)b(t)A_m(t)X^\dagger(0)b^\dagger(0)A_n(0)] \rangle_\beta, \quad (1)$$

where $A_n = a_n + a_n^\dagger + 2\lambda_n b^\dagger b$, $X = \exp[\sum_p \lambda_p (a_p^\dagger - a_p)]$, and $\lambda_p = g_{bb}/\omega_p$. Here, $\langle \dots \rangle_\beta = \mathcal{Z}^{-1} \text{Tr}(e^{-\beta H_{ph}} \dots)$ with $H_{ph} = \sum_n \omega_n a_n^\dagger a_n$. \mathcal{Z} is the phonon partition function.

The IBMA self-energy $\Sigma^{(\text{IBMA})}(t)$ can be obtained from Eq. (1) by factorizing the matrix element as

$$\begin{aligned} & \langle T[X(t)b(t)A_m(t)X^\dagger(0)b^\dagger(0)A_n(0)] \rangle_\beta \\ & \rightarrow \langle T[X(t)X^\dagger(0)] \rangle_\beta \langle T[b(t)b^\dagger(0)] \rangle_\beta \langle T[A_m(t)A_n(0)] \rangle_\beta. \end{aligned} \quad (2)$$

The product of the first two factors is recognized as the IBM Green's function. Thus, this factorization gives a result equivalent to the replacement of the bound atom Green's function

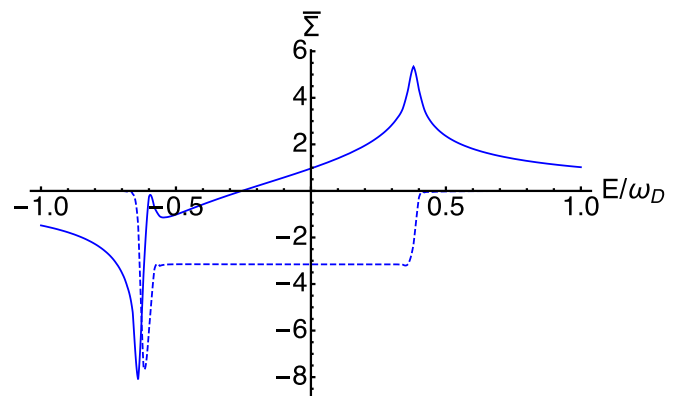


FIG. 1. Real (solid) and imaginary (dotted) parts of the atom self-energy in the IBMA $\bar{\Sigma}^{(\text{IBMA})}$ versus E/ω_D for $\epsilon = 2.0$ K. The (dimensionless) self-energy is defined $\bar{\Sigma} \equiv \Sigma/g_{kb}^2 \rho_0$ where ρ_0 is the partial (axisymmetric) vibrational density of states for the membrane.

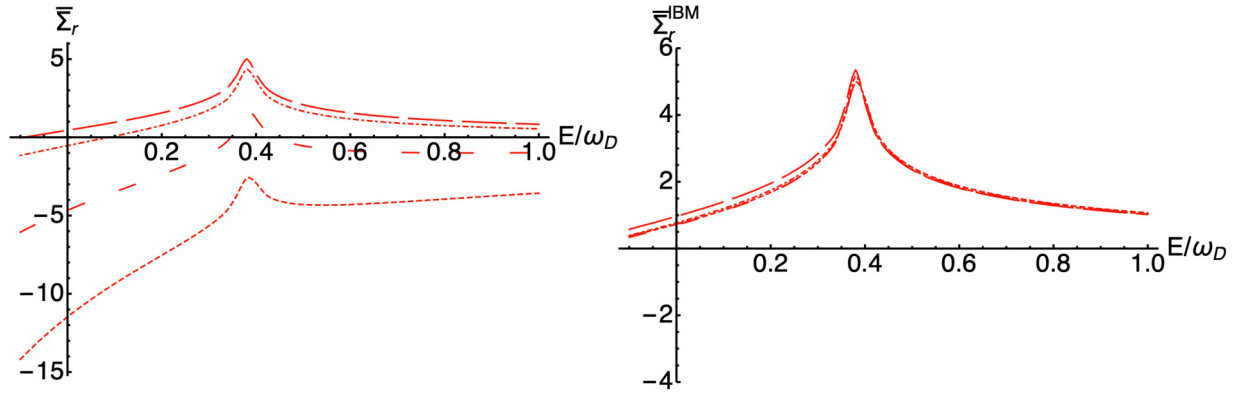


FIG. 2. Real part of the (scaled) atom self-energy $\bar{\Sigma}_r$ versus E/ω_D . IBMA (right) compares favorably to the $O(g_{kb}^2)$ (left) for $\epsilon = 2$ K (long dashed line). The real part of the $O(g_{kb}^2)$ self-energy shifts downward as ϵ is reduced: $\epsilon = 1.5$ (dot-dashed line), 1 (dashed line), and 0.8 K (short dashed line). Order $O(g_{kb}^2)$ self-energy (left) changes substantially over the range of ϵ . IBMA self-energy (right) changes little with ϵ over the same range.

by the IBM Green's function in the one-loop self-energy. The IBMA self-energy is given by (Eq. (6) in Ref. [1]),

$$\Sigma^{(\text{IBM})}(E) = g_{kb}^2 \sum_q [n_q G^{\text{IBM}}(E + \omega_q) + (n_q + 1) G^{\text{IBM}}(E - \omega_q)], \quad (3)$$

where n_q is the average number of phonons with ω_q for the membrane at temperature T and G^{IBM} is the bound atom Green's function from the independent boson model (Eqs. (28) and (29) in Ref. [1]). A plot of the real and imaginary parts of $\Sigma^{(\text{IBM})}$ as a function of the energy E is shown in Fig. 1.

There are, however, additional terms in the self-energy, beyond the IBMA terms. The most IR singular of these terms result from the noncommutativity of the displacement operator X and the phonon operator A_n as $[A_n, X] = 2\lambda_n X$. Furthermore, Wick's theorem and diagrammatic expansions based on this theorem cannot be used as the commutator is not a simple c number [7].

Disentangling the matrix element using the commutation relations yields the exact time-ordered finite temperature self-energy to order $O(g_{kb}^2)$ (and to all orders in g_{bb}). Its Fourier

transform $\Sigma(E)$ is found to be

$$\Sigma(E) = \Sigma^{(a)}(E) + \Sigma^{(b)}(E), \quad (4)$$

where

$$\begin{aligned} \Sigma^{(a)}(E) = & g_{kb}^2 \sum_q [(2\Lambda\lambda_q - 2n_q^2\lambda_q^2)G^{\text{IBM}}(E) \\ & + (n_q(2\Lambda\lambda_q + 1) + 2n_q^2\lambda_q^2)G^{\text{IBM}}(E + \omega_q) \\ & + ((n_q + 1)(1 - 2\Lambda\lambda_q) + 2n_q^2\lambda_q^2)G^{\text{IBM}}(E - \omega_q) \\ & + n_q\lambda_q^2(1 - n_q)G^{\text{IBM}}(E + 2\omega_q) \\ & - (n_q + 1)\lambda_q^2 n_q G^{\text{IBM}}(E - 2\omega_q)] \end{aligned} \quad (5)$$

$$\begin{aligned} \Sigma^{(b)}(E) = & g_{kb}^2 \sum_{p,q} [-\lambda_p\lambda_q(1 + 2n_q n_p + n_q + n_p)G^{\text{IBM}}(E) \\ & + n_q n_p \lambda_q \lambda_p G^{\text{IBM}}(E + \omega_q + \omega_p) \\ & + (n_q + 1)(n_p + 1)\lambda_q \lambda_p G^{\text{IBM}}(E - \omega_q - \omega_p) \\ & - (n_q + 1)n_p \lambda_q \lambda_p G^{\text{IBM}}(E - \omega_q + \omega_p) \\ & - (n_p + 1)n_q \lambda_q \lambda_p G^{\text{IBM}}(E + \omega_q - \omega_p)] \end{aligned} \quad (6)$$

and $\Lambda = \sum_p \lambda_p$.

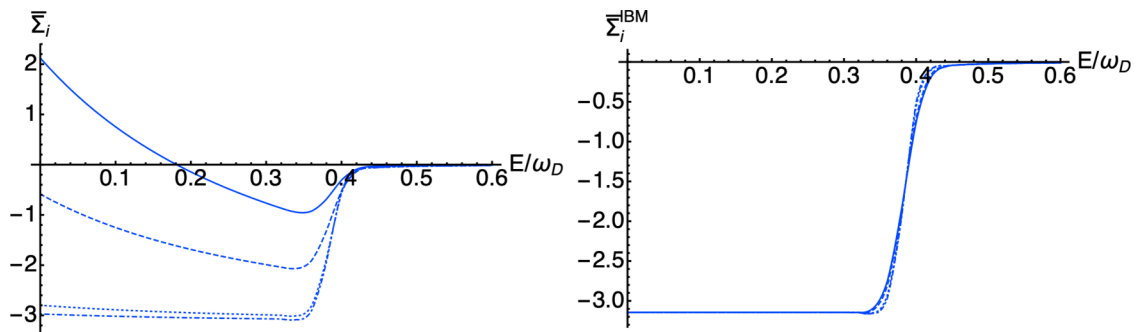


FIG. 3. Imaginary part of the atom self-energy $\bar{\Sigma}_i$ versus E/ω_D . Order $O(g_{kb}^2)$ self-energy $\bar{\Sigma}_i$ (left) becomes positive near $E = 0$ with decreasing ϵ , whereas IBMA self-energy $\bar{\Sigma}_i^{\text{IBM}}$ changes little for $\epsilon = 0.25$ (solid line), 0.3 (dashed line), 0.5 (dotted line), and 0.6 K (dot-dashed line).

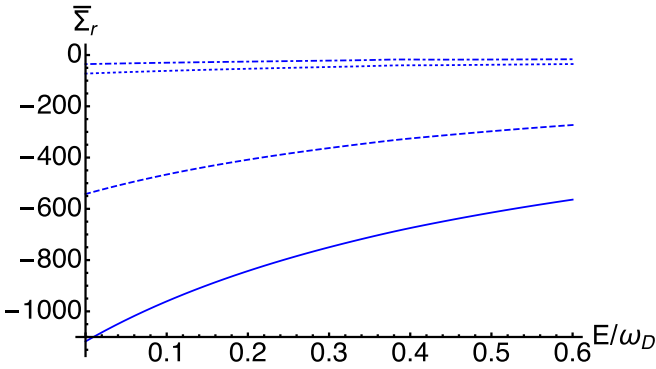


FIG. 4. Real part of the (scaled) atom self-energy $\bar{\Sigma}_r$ to order $O(g_{kb}^2)$ versus E/ω_D for $\epsilon = 0.25$ (solid line), 0.3 (dashed line), 0.5 (dotted line), and 0.6 K (dot-dashed line).

It is noted that the IBMA contributions of Ref. [1] are contained in Eq. (5); however, the additional terms beyond the IBMA dominate the self-energy at low energies for sufficiently small IR cutoff ϵ . Although the IBMA results are in agreement with the naive golden rule results ($g_{bb} = 0$) over the range of IR cutoffs considered in the numerical work of Ref. [1], the inclusion of the additional contributions contained in the $O(g_{kb}^2)$ self-energy can shift the real part of the self-energy by orders of magnitude near $E = 0$ (see Fig. 4).

Figure 2 illustrates that, for $\epsilon = 2$ K, the IBMA and the exact order $O(g_{kb}^2)$ self-energy are in good agreement over a substantial range of energies E . However, as ϵ is decreased, the real part of the self-energy Σ_r is shifted downward relative to $\Sigma_r^{(IBM)}$ near $E = 0$.

There are also substantial changes to the imaginary part of the self-energy from the additional terms. Figure 3 shows that Σ_i shifts upward near $E = 0$ with decreasing ϵ , whereas $\Sigma_i^{(IBM)}$ is insensitive to changes in ϵ .

The real part of the self-energy Σ_r at $E = 0$ is found to be negative for the values of $\epsilon \lesssim 1.5$ K, whereas $\Sigma_r^{(IBM)}(0)$ is positive over the range of ϵ considered in Ref. [1]. Analytically constructing the asymptotic expansion of Eq. (3) for $\epsilon \rightarrow 0$, it is seen that $\Sigma_r^{(IBM)}(0)$ diverges slowly (logarithmically) in the limit of $\epsilon \rightarrow 0$, a result that is not readily apparent for $\epsilon \gtrsim 0.1$ K but becomes clear with further decreases in ϵ . This result has been confirmed by numerical calculations. In contrast, the real part of the order $O(g_{kb}^2)$ self-energy at $E = 0$, $\Sigma_r(0)$, diverges more rapidly (algebraically) as $\epsilon \rightarrow 0$. This rapid descent of $\Sigma_r(0)$ with decreasing ϵ is clearly visible for $\epsilon \lesssim 0.5$ K as seen in Fig. 4.

It is also noted that the curvatures of the real self-energies differ in sign with the real part of exact order $O(g_{kb}^2)$ self-energy found to be concave down, whereas the corresponding IBMA self energy is concave up. It will be seen graphically that this change in the curvature at low energies becomes relevant in using SPA to determine the adsorption rate.

SPA assumes that the atom Green's function has a simple pole in the lower half of the complex energy plane that is located close to the real axis. By linearizing the self-energy about an assumed quasiparticle energy E_p , one obtains that E_p is determined by

$$E_p - E_k = \Sigma_r(E_p). \quad (7)$$

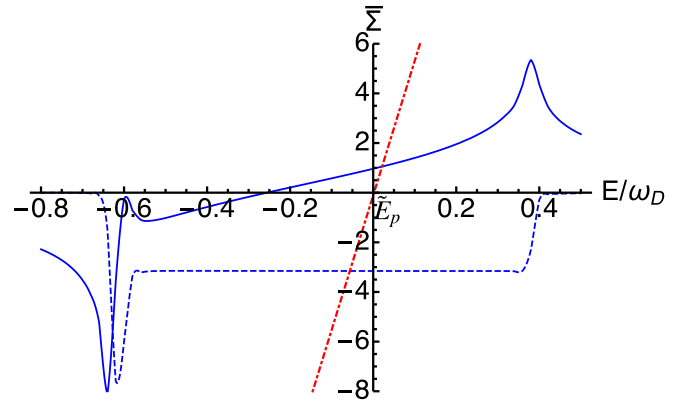


FIG. 5. Graphical solution for the quasiparticle energy E_p . Real part (solid line) of the atom self-energy in IBMA $\text{Re } \bar{\Sigma}^{(IBM)}$ for $\epsilon = 2.0$ K versus E/ω_D crosses the line (dot-dashed line) where $\bar{E}_p - \bar{E}_k = \text{Re } \bar{\Sigma}(\bar{E}_p)$. In the single-pole approximation, the adsorption rate depends on $\text{Im } \Sigma^{(IBM)}(E_p)$ and is determined by Eq. (8).

The adsorption rate Γ would then be given by

$$\Gamma \approx -2Z\Sigma_i(E_p), \quad (8)$$

where the quasiparticle weight $Z = (1 - \frac{\partial \Sigma_r(E)}{\partial E}|_{E=E_p})^{-1}$.

One can solve Eq. (7) graphically (see Fig. 5). For sufficiently large ϵ , I find there is a self-consistent solution to Eq. (7); however, with the large shift in the real part of the order $O(g_{kb}^2)$ self-energy Σ_r at low ϵ , I find that a self-consistent solution to Eq. (7) does not exist for $\epsilon \lesssim 0.4$ K (see Fig. 6). Thus, the SPA cannot be used to obtain an approximate adsorption rate in this case.

To summarize, the IBMA self-energy is a poor approximation to the exact self-energy to order $O(g_{kb}^2)$ for micrometer-sized samples of suspended graphene. For $\epsilon \sim 1.7$ K, the magnitude of terms neglected in the IBMA self-energy

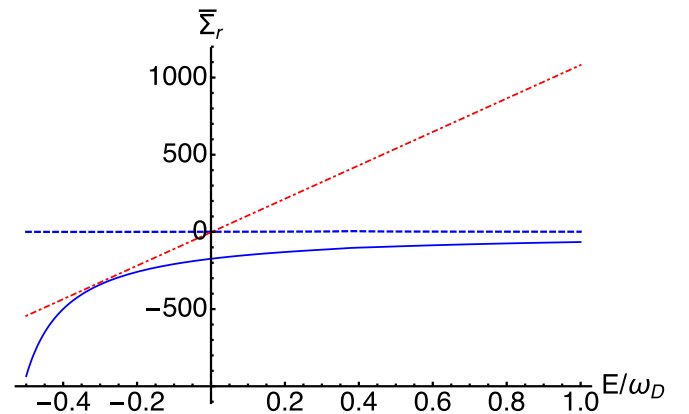


FIG. 6. Graphical solution for the quasiparticle energy E_p fails with large negative shifts of the real part of the self energy. Real part (solid line) of the atom self-energy $\text{Re } \bar{\Sigma}$ for $\epsilon \leq 0.4$ K versus E/ω_D does not intersect with the line (dot-dashed line) where $\bar{E}_p - \bar{E}_k = \text{Re } \bar{\Sigma}(\bar{E}_p)$. The single-pole approximation fails for low atom energy [$E_k < |\Sigma_r(0)|$] when using the order $O(g_{kb}^2)$ self-energy but does not using the IBMA self-energy (horizontal dashed line).

exceeds the magnitude of IBMA self-energy at zero energy. (This value of ϵ corresponds to a membrane radius $a \sim 0.07 \mu\text{m}$).

Using the order $O(g_{kb}^2)$ self-energy, there are no solutions to Eq. (7) for the self-consistent quasiparticle energy E_p for sufficiently small ϵ . Thus, the use of the SPA in this regime is invalid when using the order $O(g_{kb}^2)$ self-energy. The disagreement of the results of Ref. [1] with previous work is a

consequence of the use of the IBMA self-energy which does not contain the additional contributions essential to capturing the behavior at low ϵ .

This work received support under NASA Grant No. 80NSSC19M0143. The hospitality of JILA and the partial support of a JILA Visiting Fellowship are also gratefully acknowledged.

-
- [1] S. Sengupta, *Phys. Rev. B* **100**, 075429 (2019).
[2] D. P. Clougherty, *Phys. Rev. B* **90**, 245412 (2014).
[3] G. D. Mahan, *Many-Particle Physics* (Plenum, New York, 1981).
[4] Y. Zhang and D. P. Clougherty, *Phys. Rev. Lett.* **108**, 173202 (2012).

- [5] D. P. Clougherty and Y. Zhang, *Phys. Rev. Lett.* **109**, 120401 (2012).
[6] D. P. Clougherty, *Phys. Rev. B* **96**, 235404 (2017).
[7] A. L. Fetter and J. D. Walecka, *Quantum Theory of Many-Particle Systems* (Dover, Mineola, NY, 2003).